OAK RIDGE
NATIONAL LABORATORY
MANAGED BY UT-BATTELLE
FOR THE DEPARTMENT OF ENERGY

ORNL/TM-2010/223

Pre- and Post-Irradiation Characterization and Properties Measurements of ZrC-coated Surrogate TRISO Particles

Gokul Vasudemurthy, Yutai Katoh, John D. Hunn, and Lance L. Snead

September 2010

UT-BATTELLE
ORNL-27 (4-00)

Pre- and post-irradiation characterization and properties measurements of ZrC coated surrogate TRISO particles

Gokul Vasudevamurthy, Yutai Katoh, John D. Hunn and Lance L. Snead
Oak Ridge National Laboratory, Oak Ridge, TN, USA

Summary
Zirconium carbide is a candidate to either replace or supplement silicon carbide as a coating material in TRISO fuel particles for high temperature gas-cooled reactor fuels. Six sets of ZrC coated surrogate microsphere samples, fabricated by the Japan Atomic Energy Agency using the fluidized bed chemical vapor deposition method, were irradiated in the High Flux Isotope Reactor at the Oak Ridge National Laboratory. These developmental samples available for the irradiation experiment were in conditions of either as-fabricated coated particles or particles that had been heat-treated to simulate the fuel compacting process. Five sets of samples were composed of nominally stoichiometric compositions, with the sixth being richer in carbon (C/Zr = 1.4). The samples were irradiated at 800 and 1250°C with fast neutron fluences of 2 and 6 dpa. Post-irradiation, the samples were retrieved from the irradiation capsules followed by microstructural examination performed at the Oak Ridge National Laboratory's Low Activation Materials Development and Analysis Laboratory. This work was supported by the US Department of Energy Office of Nuclear Energy's Advanced Gas Reactor program as part of International Nuclear Energy Research Initiative collaboration with Japan. This report includes progress from that INERI collaboration, as well as results of some follow-up examination of the irradiated specimens. Post-irradiation examination items included microstructural characterization, and nanoindentation hardness/modulus measurements. The examinations revealed grain size enhancement and softening as the primary effects of both heat-treatment and irradiation in stoichiometric ZrC with a non-layered, homogeneous grain structure, raising serious concerns on the mechanical suitability of these particular developmental coatings as a replacement for SiC in TRISO fuel. Samples with either free carbon or carbon-rich layers dispersed in the ZrC coatings experienced negligible grain size enhancement during both heat treatment and irradiation. However, these samples experienced irradiation induced softening similar to stoichiometric ZrC samples.

1.0 Description of the Experiment

The developmental samples used in the irradiation experiment consisted of yttria-stabilized zirconia kernels coated with an inner pyrocarbon layer followed by a ZrC coating. Table 1 shows the sample irradiation matrix used in this experiment. Some of the sample lots had an additional outer pyrocarbon layer, as indicated in Table 1. The details of the coating process and the prevailing conditions are discussed by Aihara et. al. [1-3]. Around fifty spheres from each of the sample lots were randomly selected for the irradiation experiment. Irradiation was performed in the High Flux Isotope Reactor (HFIR) at Oak Ridge National Laboratory (ORNL) during 2008-09. After irradiation, the samples were retrieved from the capsules and sorted in a hot cell at the ORNL Irradiated Materials Examination and Testing (IMET) facility. Gamma spectroscopy was performed to indentify the major activation products and the dose rates at contact and 30 cm from the retrieved specimens were measured. The specimens were sorted and shipped to the Low Activation Materials Development and Analysis (LAMDA) Laboratory for post-irradiation

examination (PIE). During particle sorting, an initial estimation of the coating failure of the irradiated specimens was performed. The sorted samples shipped to LAMDA were gently cleaned in an ultrasonic bath and mounted in a two part epoxy resin. The cured sample mounts were then ground using silicon carbide paper followed by stepwise polishing using polycrystalline diamond solutions. The samples were subsequently examined using Phillips XL-30 and JEOL 6500F field emission gun scanning electron microscopes (FEG-SEM). The process flow diagram is shown in Figure 1. Nanoindentation hardness and modulus were measured on all six unirradiated and irradiated samples using an MTS Nanoindenter™ XP system.

Table 1. Sample Matrix and Experimental conditions.

Sample Lot	IPyC/OPyC	C/Zr	Dose (dpa)	T_{irr} (°C)
ZrC-06-2003HT	Yes/No	1.4	2	800, 1250
			6	1250
ZrC-06-2048HT	Yes/No	1.0	2	800, 1250
			6	1250
ZrC-07-3002	Yes/Yes	1.0	2	800, 1250
			6	1250
ZrC-07-3002HT	Yes/Yes	1.0	2	800, 1250
			6	1250
ZrC-07-3010	Yes/Yes	1.0	2	800, 1250
			6	1250
ZrC-07-3010HT	Yes/Yes	1.0	2	800, 1250
			6	1250

** Indicates nominal values, ¥ 1 dpa (displacement per atom) per 1×10^{25} neutrons/m^2 (E >0.1MeV)*
Suffix HT indicates Heat-treated samples

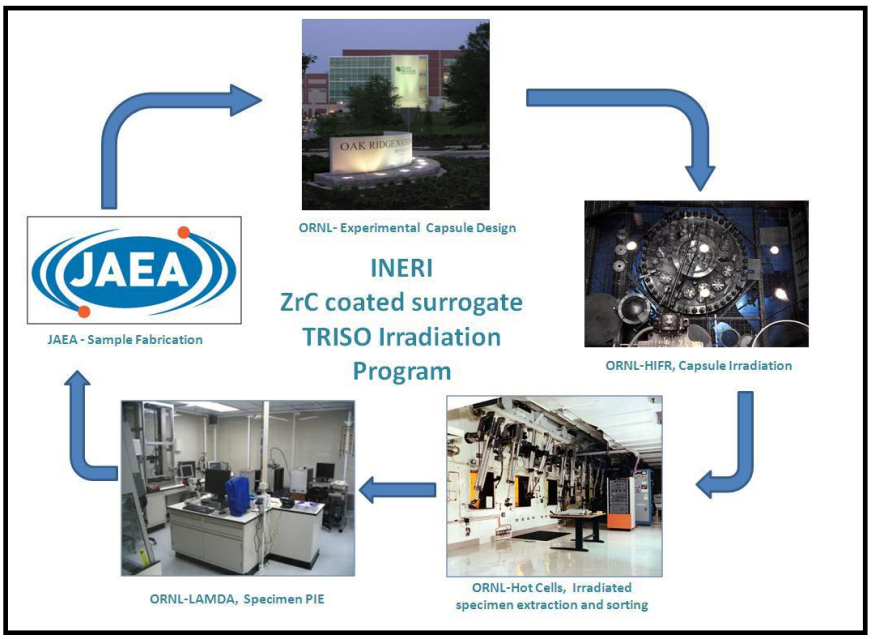

Fig. 1. Current program process flow.

2.0 Post-Irradiation Preliminary Observation at IMET

ZrC coated spheres extracted from the irradiation capsules at the ORNL-IMET facility were visually inspected to assess the extent of macro-scale damage to the coatings. This exercise traditionally forms the first step of post-irradiation evaluation before transporting the samples to LAMDA laboratory for further detailed analyses. Initial inspection of irradiated samples using a Kollmorgen periscope during extraction and sorting showed significant differences in the coating integrity/intactness between the 2 dpa at 800°C, 2 dpa at 1250°C, and 6 dpa at 1250°C samples.

The majority of 2 dpa samples showed coating failure (broken or chipped coatings) regardless of the irradiation temperature. Statistically, more samples irradiated at 2 dpa at 800°C had damaged coatings than samples irradiated to 2 dpa at 1250°C. In addition, samples irradiated to 6 dpa at 1250°C had a lower fraction of broken/chipped coatings, in comparison with the 2 dpa samples. The reason for this damage was not resolved and could only be attributed in part to structural damage during handling of the 2 dpa samples prior to or after irradiation. Similar instances of coating damage were observed during sample preparation, where the 2 dpa samples suffered from dislodged grains. This damage could not be clearly attributed to irradiation effects. The statistics are shown in Tables 2 and 3 for the particles irradiated to 2 and 6 dpa, respectively. Figures 2 through 6 are representative images of particles with damaged and intact coatings. The differentiation between damaged and intact particles in a particular lot was only possible by visual distinction of the size of the particles in the sorting tray. Since the resolution of the viewing system was limited, it was not clear whether the damage was limited to the outer pyrocarbon layer or the actual ZrC layer.

Under these limitations of resolution in the inspection periscope, the 2 dpa specimens seemed to have undergone a higher degree of coating damage than the rest, as evidenced by the coating debris found along with the particles in the sorting tray. No detectable debris was found in the sorting trays of particles irradiated to 6 dpa, except in sample lot 2048HT (Fig. 5). The particles irradiated to 6 dpa were distinguished based on their appearance. Some of the particles appeared carbonaceous while others appeared metallic (Fig. 6). The metallic ones were assumed to have lost their outer pyrocarbon layers since no debris indicative of the damaged ZrC layer was found in the sorting trays. However, particles in sample lot 2048HT irradiated to 6 dpa showed a high degree of coating damage as evidenced by the debris in the sorting tray. Based on this observation, it was concluded that particles of lot 2048HT appearing carbonaceous had lost their ZrC coating and were appearing dark due to exposure of the inner pyrocarbon layer.

Table 2. Initial estimates on samples irradiated to 2 dpa.

Sample Lot	OPyC	T_{irr} (°C)	Total Number of Microspheres counted	Size 1	Size 2	Failure (%)
3002	Yes	800	47	37	10	78.7
2003HT	Yes	800	31	8	23	25.8
3002HT	Yes	1250	36	0	36	0.0
2003HT	No	1250	44	17	27	38.6
3010	Yes	1250	47	12	25	46.8
2048HT	No	1250	45	1	44	2.2

Size 1 represents particles with either damaged OPyC and/or ZrC coating
Size 2 represents particles with intact coating

Table 3. Initial estimates on samples irradiated to 6 dpa.

Sample Lot	OPyC	T_{irr} (°C)	Total Number of Microspheres counted	Metallic	Carbonaceous
3002	Yes	1250	50	17	33
3002HT	Yes	1250	49	13	36
3010	Yes	1250	48	20	28
3010HT	Yes	1250	44	15	29
2003HT	No	1250	54	0	54
2048HT	No	1250	48	12	36

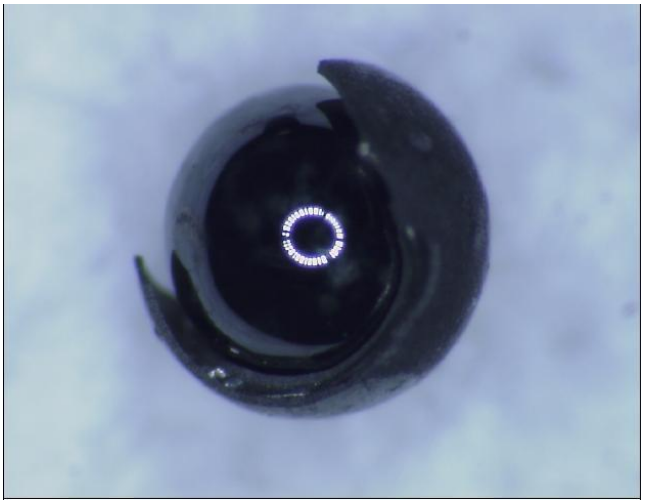

Fig. 2. Irradiated particle from 3010 sample lot showing damaged coating (2 dpa, 800°C).

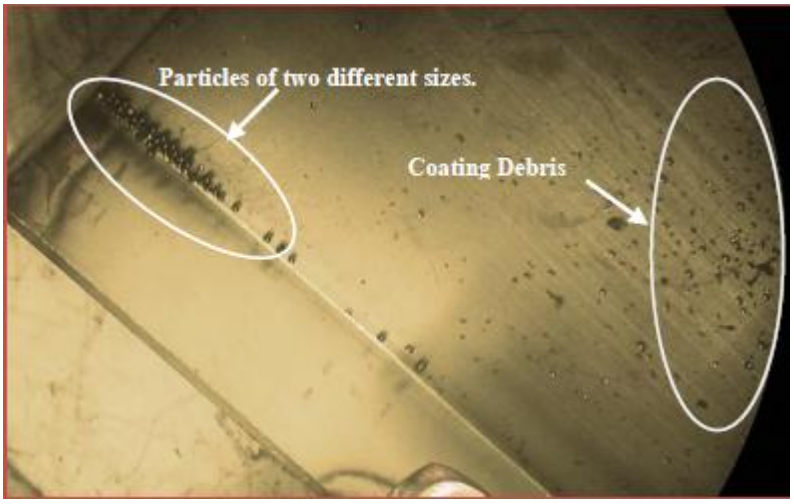

Fig. 3. Irradiated particles from 3002 sample lot showing two sizes and coating debris (2 dpa, 800°C).

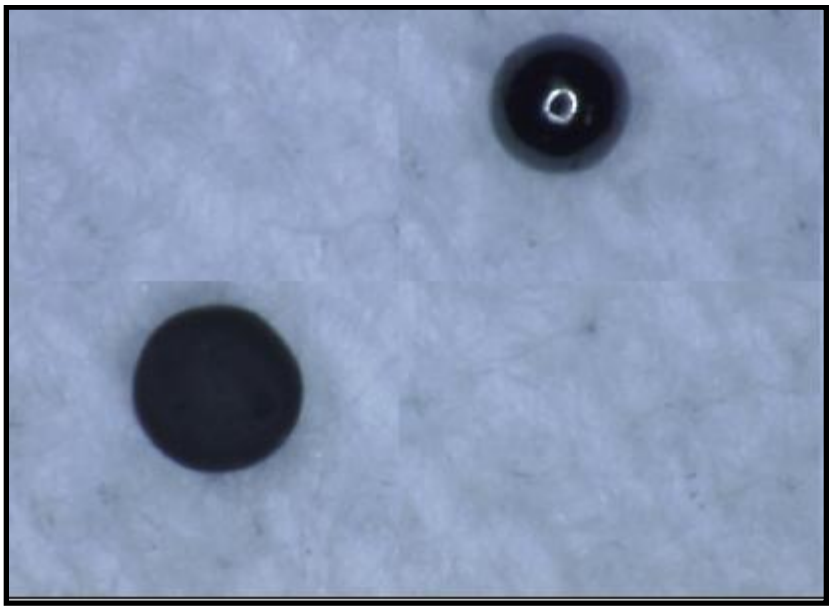

Fig. 4. Two irradiated particles (two sizes, one with intact on the left and one with damaged coating on the right) from 3002 sample lot as received at LAMDA (2 dpa, 800°C).

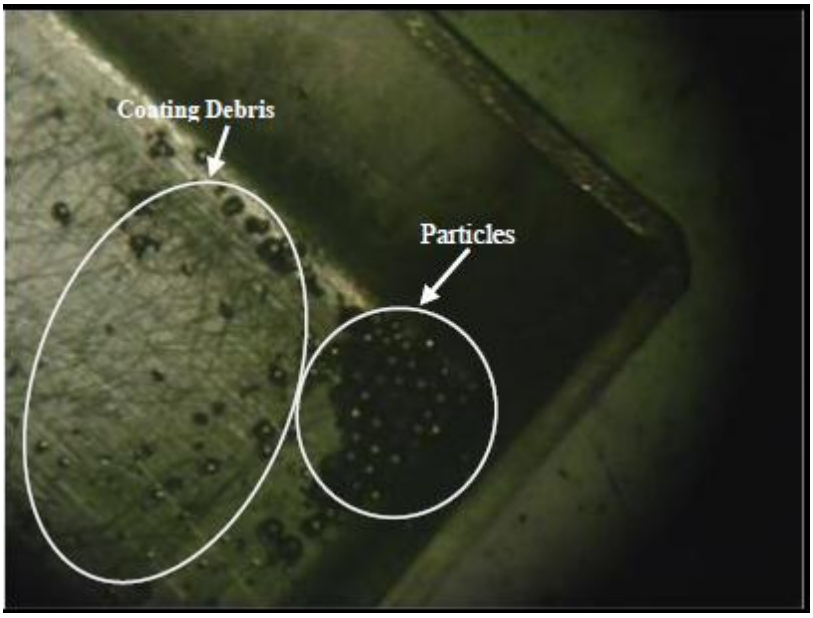

Fig. 5. Sample 2048HT irradiated to 6 dpa at 1250°C showing metal like and carbonaceous particles, along with coating debris.

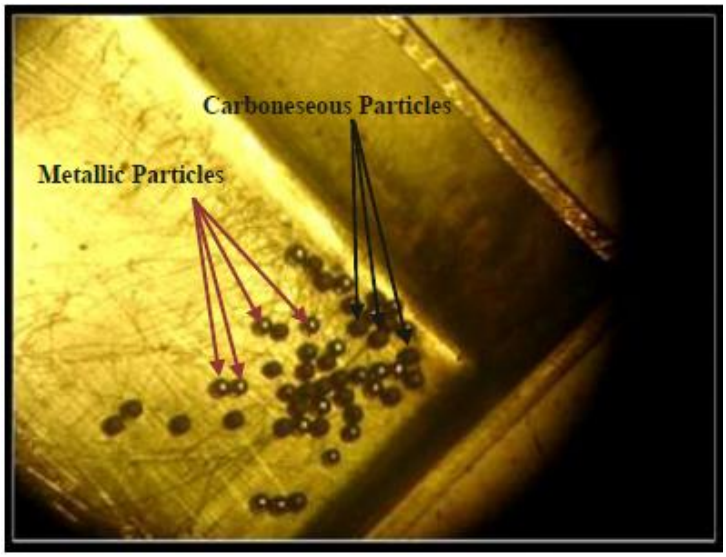

Fig. 6. Samples 3002 irradiated to 6 dpa at 1250°C showing metal like and carbonaceous particles.

3.0 Microstructural Observations

3.1 Pre-Irradiation Microstructure of As-fabricated & Heat-treated Samples

The experiment included the irradiation of two as-fabricated samples and four heat-treated samples as listed in Table 1. Out of the six sample sets, samples 3010HT and 3002HT were derived from samples 3010 and 3002, after heat-treating the respective as-fabricated samples at ~1800°C for 1h to simulate the effect of heat-treating during a typical fuel compacting process.

Figure 7 shows the representative pre-irradiation microstructure of the as-fabricated and heat treated particles. Sample 3002 showed very small grains (<100 nm) with no clear layered structure. The grains were homogenous and the micrograph showed a dense microstructure with the presence of very few voids, typical of the material fabricated by the CVD process. Sample 3002HT, produced from sample 3002 following heat-treatment, showed the presence of large grains (> 3 μm) in addition to some pores. The observed grain size enhancement and pore evolution is attributed to the heat-treatment step. Sample 3002HT did not show a layered structure.

The as-fabricated sample 3010 showed a layered structure with very small grains similar to the sample 3002, but with higher porosity. A higher magnification micrograph (Fig. 8) showed alternating dark and bright bands indicating the presence of free carbon or carbon-rich layers between the ZrC layers, as indicated by the backscattered electron micrographs.

A comparison of 3002HT, 3010HT and 2048HT, all heat-treated and with nominal stoichiometry of 1.0, showed significantly different microstructures. Sample 3010HT, which was derived from sample 3010 following heat-treatment, showed the formation of fairly homogeneous grains similar, but smaller in size, than the grains of 3002HT. The microstructure of sample 3010HT also showed higher porosity compared to other heat-treated samples. The grains in samples 3002HT and 3010HT did not exhibit any particular pattern, whereas sample 2048HT clearly showed a bi-layered structure with annular grain bands in the inner region. The region close to

the IPyC-ZrC layer interface contained finer grains compared to the region close to the outer periphery. This distinctive structure is attributed in part to possible changes in processing conditions during this particular coating run resulting in layers with different carbon compositions. However, no such changes were intended or noted during the deposition. This conclusion is further supported by the micrograph (Fig. 9) of Sample 2048 (not irradiated in this experiment). This as-fabricated predecessor of sample 2048HT shows a clear layered structure in the inner region which had been retained during heat-treatment. Post heat-treatment, the inner region with finer grains had undergone grain size enhancement on a smaller scale compared to the outer layer. This anomaly could be attributed to the presence of a carbon-rich layer between the ZrC layers in the inner region, which could not be analytically distinguished due to limitations in the resolution of the back scattered electron images and energy dispersive spectroscopy. This hypothesis was confirmed from the microstructural observations of the known carbon-rich sample 2003HT (Fig. 7). The microstructure of this sample revealed a ring structure with alternating dark and bright annular bands similar to, but more conspicuous and clear compared to sample 3010HT. The dark bands represented the excess carbon or carbon-rich layer deposited between the coating layers, while the bright bands represented small ZrC grains (~100 nm). The presence of carbon-rich layers was also confirmed by the Japan Atomic Energy Agency (JAEA) work, reporting the transmission electron microscope observations of the heat-treated samples of 2003HT [1- 3]. The presence of the carbon interlayer seemingly inhibited grain growth in sample 2003HT during heat-treatment. Extending the observations, it could be concluded that although samples 3002HT, 3010HT and 2048HT were expected to have a nominal stoichiometric composition, it was clear that the inner region of sample 2048HT and all of 3010HT had carbon-rich layers deposited between the coating layers, which resulted in stunted grain enhancement (Fig. 7). It is noted here that the stark variation in the microstructure indicates variation in parameters between coating runs. This was due to the fact that the ZrC CVD coating process at JAEA was still developmental at the time of the study. One of the goals of this experiment was to study the variation in irradiation response with varying microstructure and composition resulting from such developmental CVD runs. Although the bulk stoichiometry of all the nominally stoichiometric samples was measured to be 1.0, carbon-rich layers were found in all samples except 3002HT.

3.2 Irradiated Microstructure

Observations of sample 3002 (Fig. 10) revealed no significant change from the pre-irradiation coating microstructure, with no noticeable change in grain size or porosity. Although some microcracks were observed close to the IPyC layer, they could not be clearly attributed to irradiation and could be artifacts of the specimen preparation.

Micrographs of sample 3002HT (Fig. 11) indicated no drastic changes in the microstructure compared to the pre-irradiation microstructure. Modest grain size enhancement was observed, especially in the inner layers close to the ZrC-IPyC interface in samples irradiated to 6 dpa. Most of the porosity in these samples appeared to have resulted from coalescence of grains, commonly observed during heat-treatment and were possibly preserved during irradiation. The extent of porosity evolution during irradiation was unclear.

The irradiated microstructure of sample 2048HT (Fig. 12) revealed a preserved pre-irradiation two region layered structure. Grain enhancement phenomenon similar to 3002HT was observed in these samples and was more clearly visible in samples irradiated to 2 dpa at 800°C. Grain size enhancement in most of the annular bands of the inner regions, which had carbon-rich layers

between them, appeared to be on a much smaller scale, except in areas in the immediate vicinity of the IPyC-ZrC interface. It is noted here that the reason for more visible grain structure in the fine grained unirradiated specimens is due to etching by a diluted 10% hydrofluoric - 20% nitric acid mixture. However the irradiated specimens were not subject to etching due to handling issues.

Micrographs of sample 3010 irradiated at 2 and 6 dpa (Fig. 13) showed grain growth similar to the inner region of 2048HT indicating the presence of a carbon-rich layer between the ZrC layers. Sample 3010HT (Fig. 14) showed the preservation of pre-irradiation porosity with a modest (in comparison to 3002HT) grain growth similar to the irradiation induced grain growth in the inner region of sample 2048HT.

The microstructure of sample 2003HT (Fig. 15) did not show any noticeable changes in terms of grain size enhancement or formation of porosity. The carbon-rich layer between the ZrC layers had clearly suppressed grain size enchantment in these samples. All the 2003HT samples retained the pre-irradiation layered structure.

3.3 Conclusions of Microstructural Observations

As-fabricated and Heat-treated Microstructures

Samples with as-fabricated non-layered microstructure experienced severe grain size enhancement during heat-treatment by grain coalescence, whereas samples with as-fabricated layered microstructure exhibited much smaller degree of grain size enhancement. This is attributed to the presence of carbon-rich layers deposited between the ZrC layers during fabrication. The role of the carbon-rich layer in inhibiting grain size enhancement was confirmed during subsequent microstructural observations of the known carbon-rich 2003HT samples, which indicated no significant grain enhancement after heat-treatment. Further, the coating with nominally stoichiometric ZrC (2048HT) had a distinctive bi-layer microstructure, indicating change in coating condition in the middle of this particular coating run. The as-fabricated and nominally stoichiometric sample 3010 showed alternating dark and light bands similar to carbon-rich 2003HT. Sample 3010HT derived from sample 3010 showed a lesser degree of grain size enhancement compared to 3002HT and the outer region of 2048HT. This was again attributed to the presence of carbon-rich layers in between the ZrC coating layers which was observed in the as-fabricated sample 3010.

Irradiated Microstructures

Samples without a layered structure had undergone a modest grain size enhancement during irradiation, which is expected to contribute to further degradation in mechanical strength. Samples with a layered structure and nominally stoichiometric compositions (2048HT, 3010HT) experienced a lesser degree of grain growth during irradiation, similar to the effect of heat-treatment. The effects of irradiation in some of the regions were similar to carbon-rich ZrC (2003HT). The stunted grain growth observed in some of the regions is attributed to the presence of carbon-rich interlayers, a hypothesis confirmed from the microstructural observation of irradiated sample 2003HT, which showed no change in pre-irradiation microstructure, an effect clearly attributable to the presence of excess carbon between layers. This effect was very similar to that of the heat-treatment in these samples. Although there was evidence of large pores in some of the irradiated samples, it was unclear if the pores had originated during heat-treatment or irradiation as no quantitative analysis was possible.

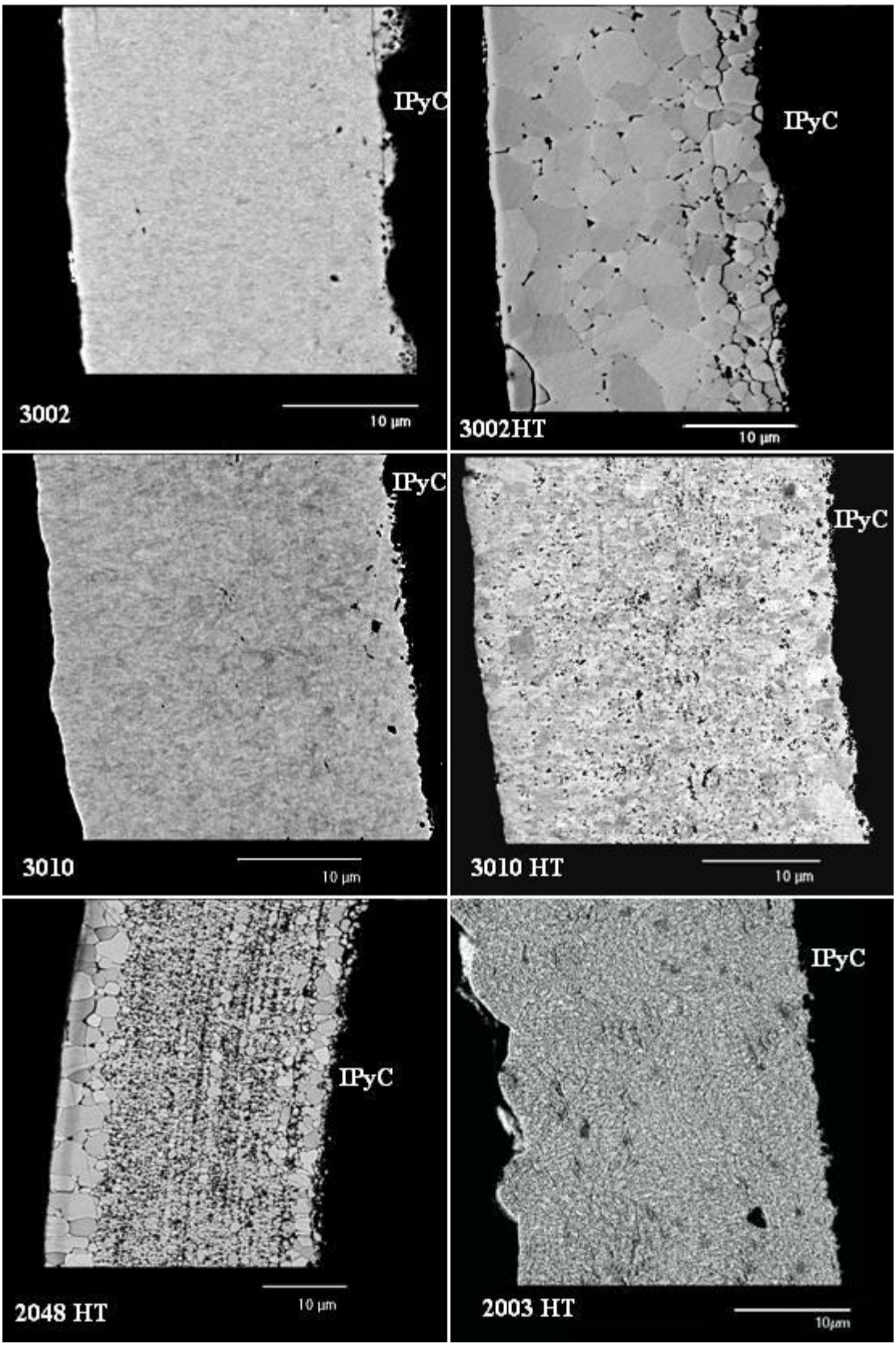

Fig. 7. Microstructures of as-fabricated and heat-treated samples (unirradiated).

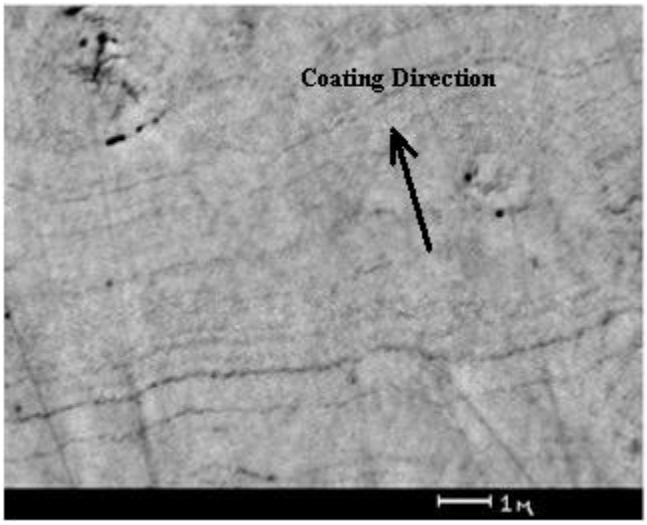

Fig. 8. Microstructure of Sample 3010, showing light and dark bands.

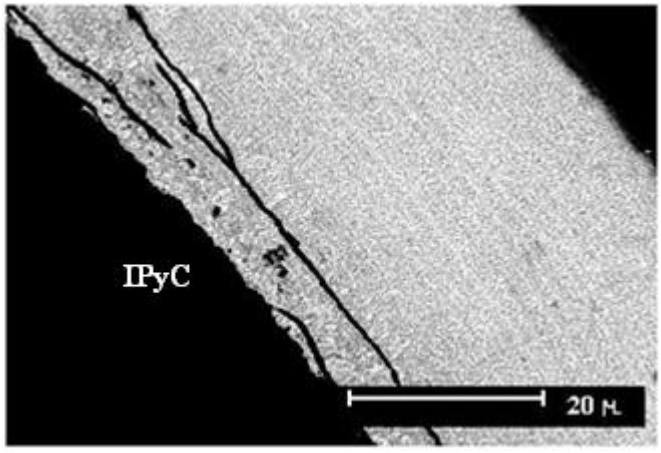

Fig. 9. Microstructure of Sample 2048 (precursor of 2048HT).

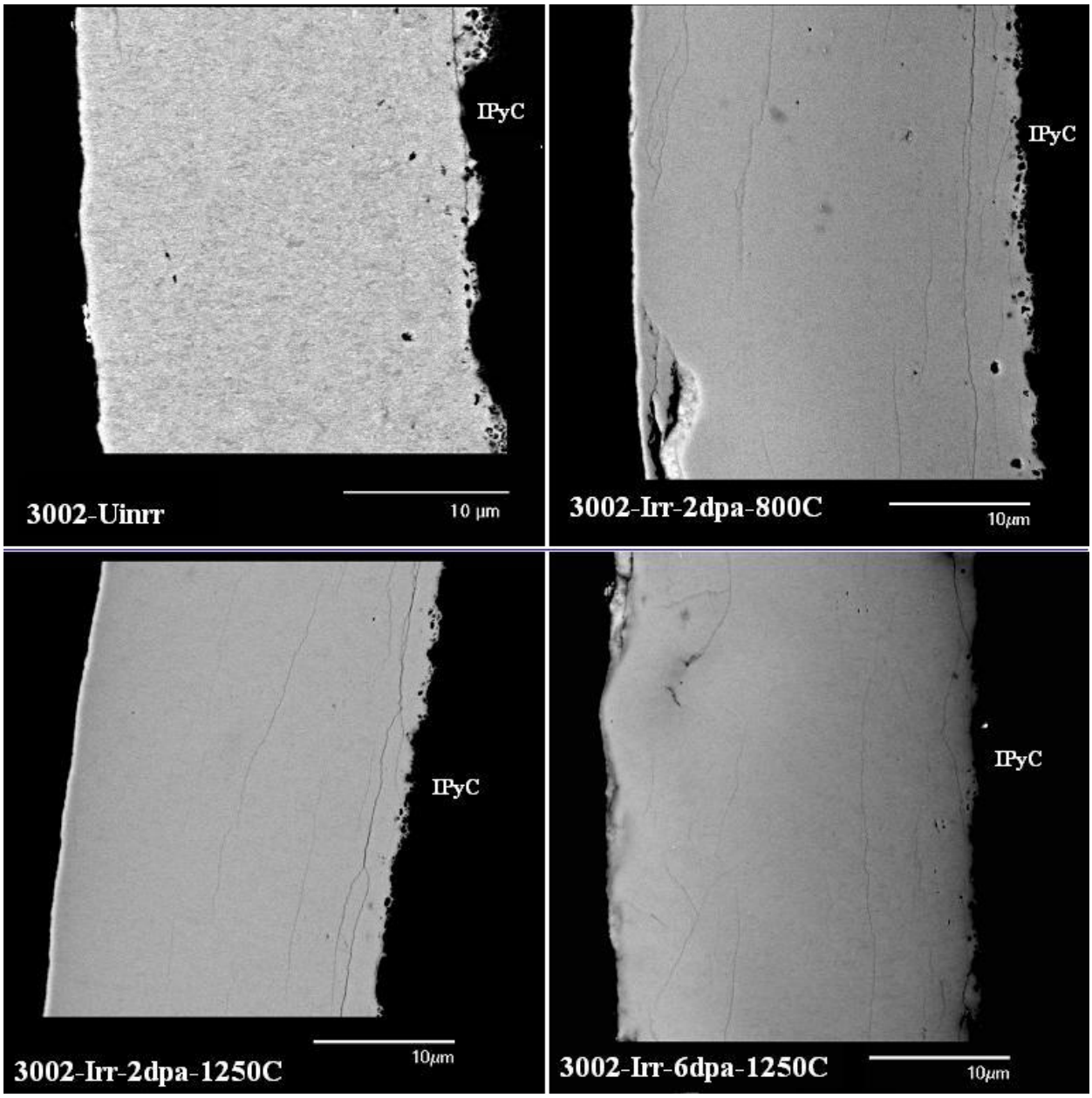

Fig. 10. Microstructure of Sample 3002.

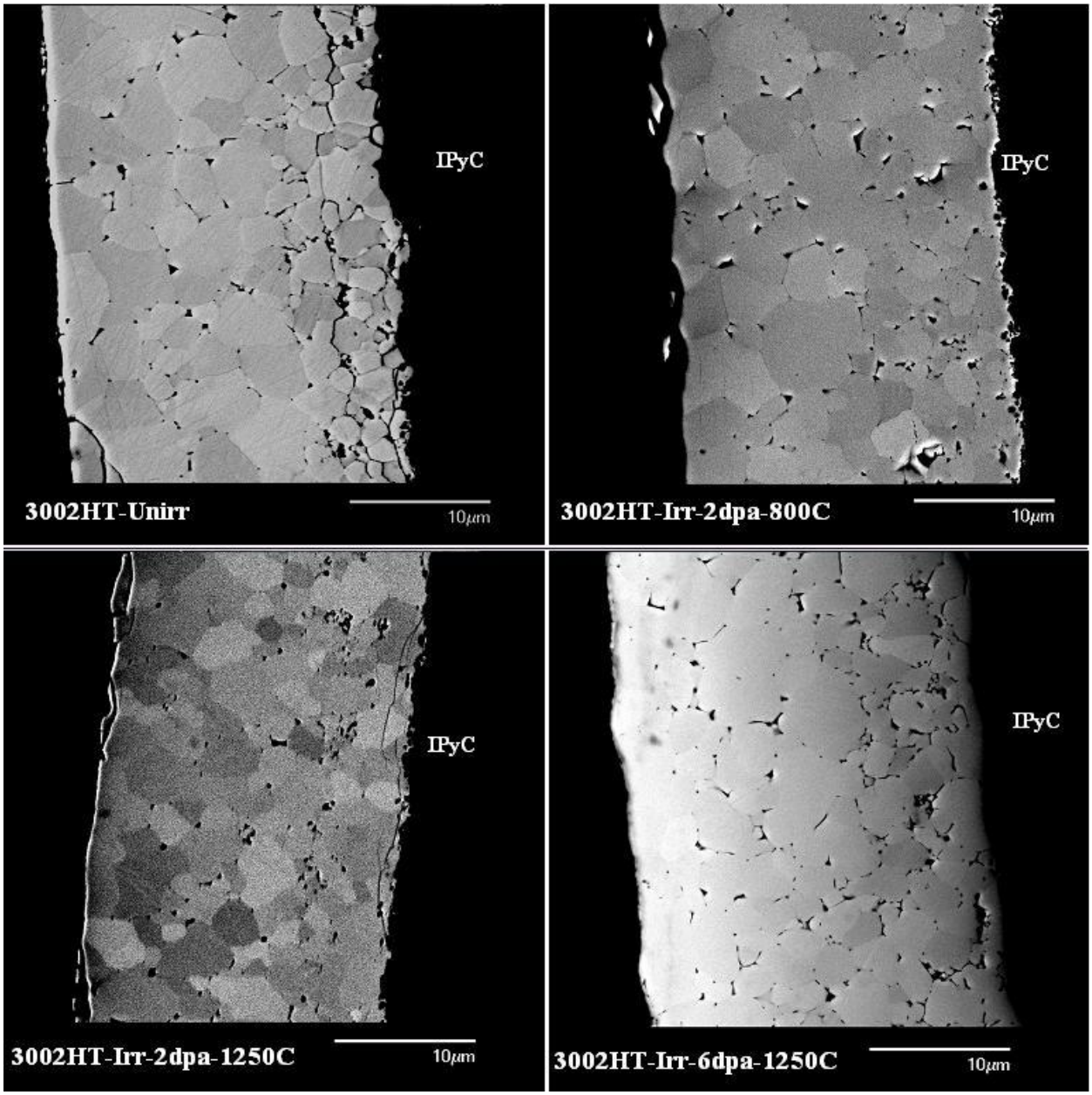

Fig. 11. Microstrucrtre of Sample 3002HT.

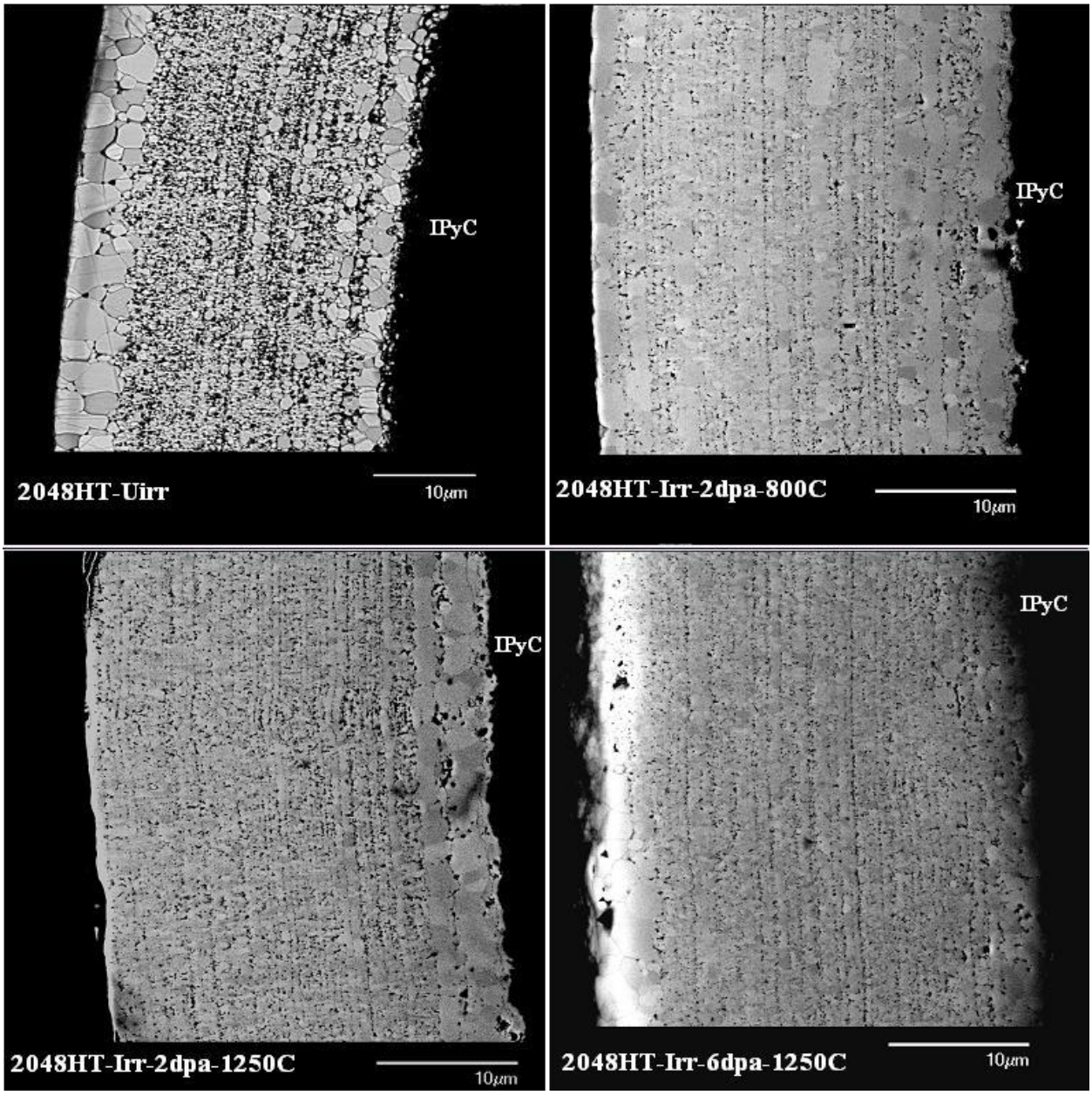

Fig. 12. Microstructure of Sample 2048HT.

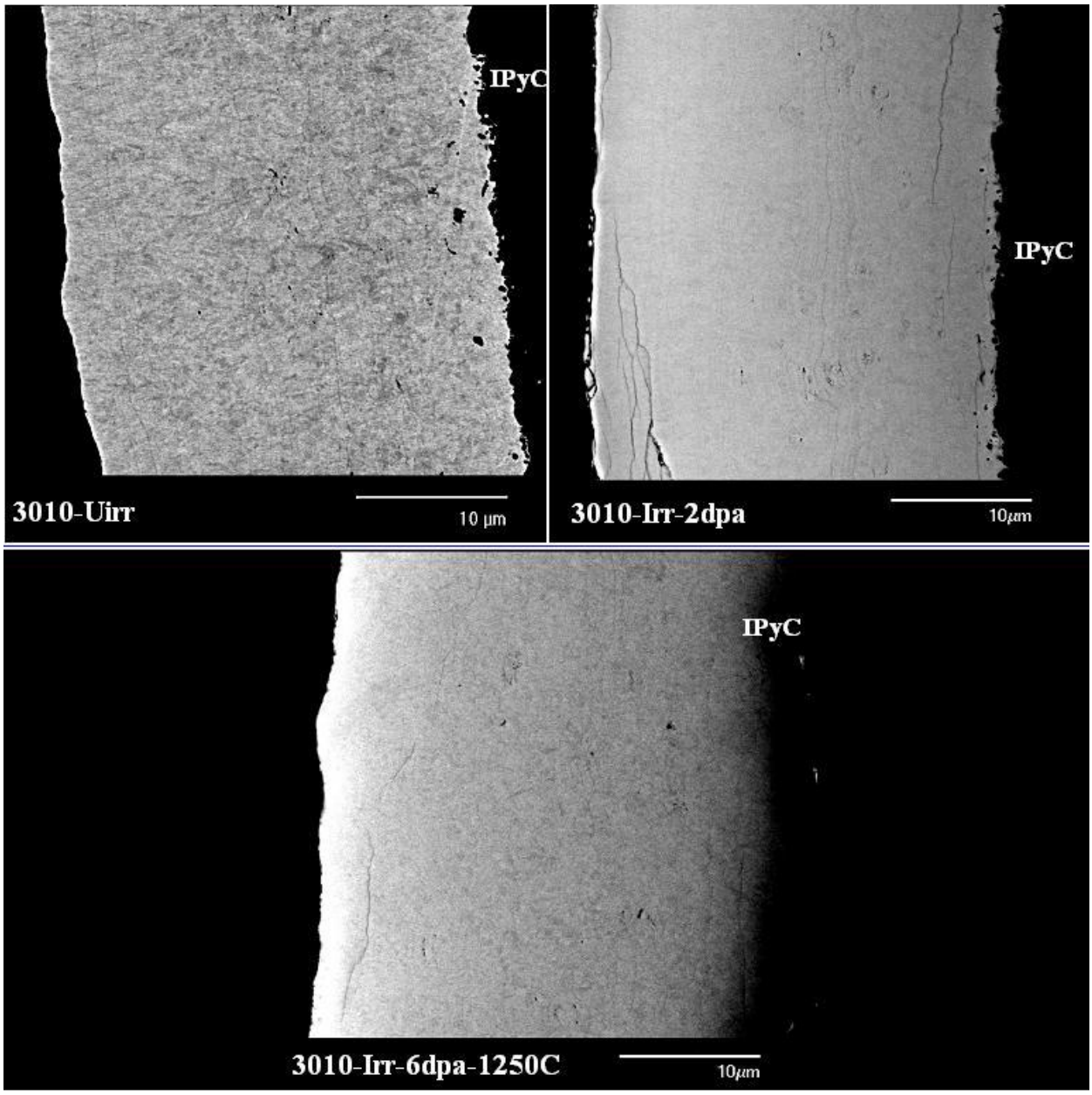

Fig. 13. Microstructure of Sample 3010.

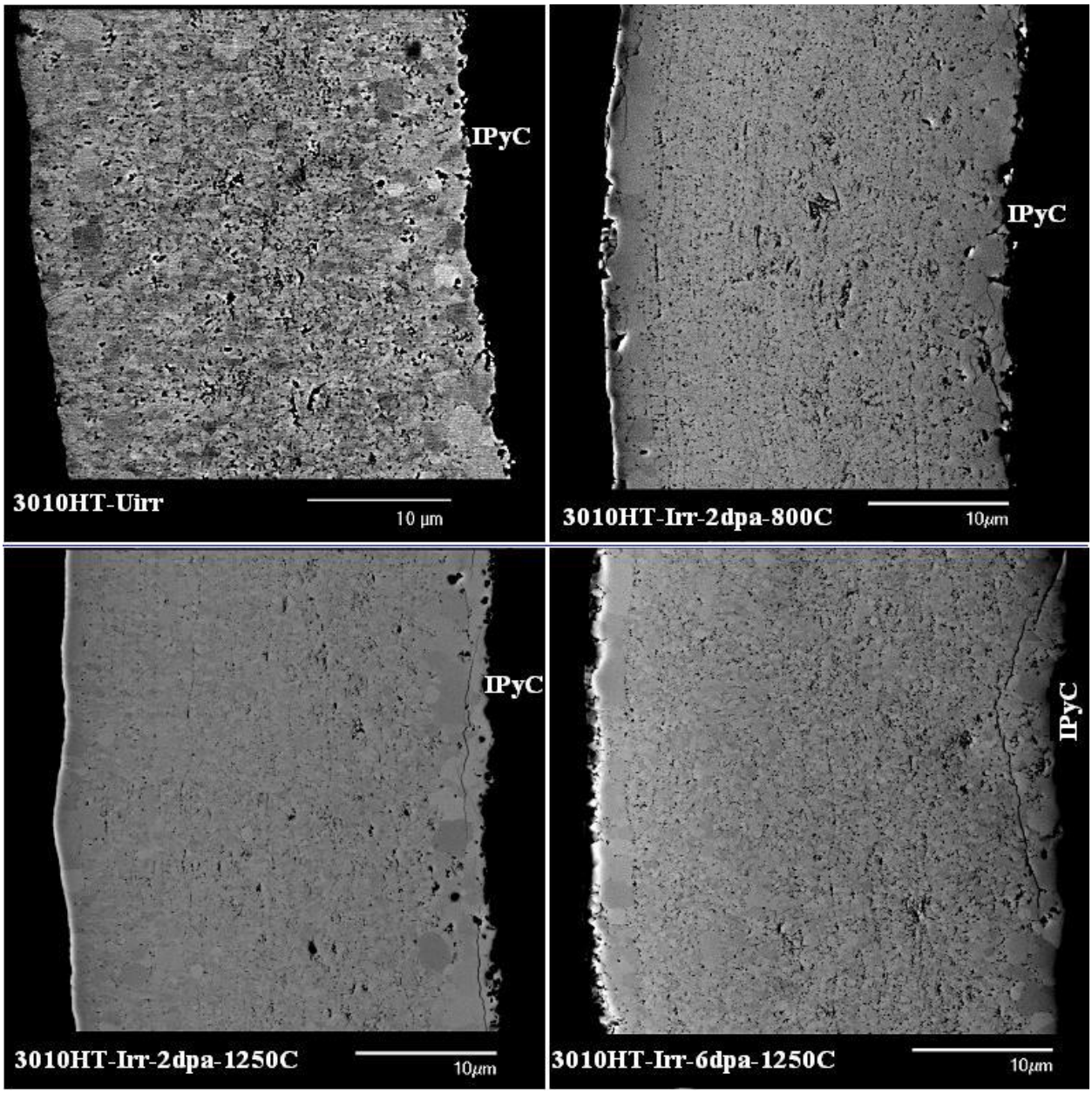

Fig. 14. Microstructure of Sample 3010HT.

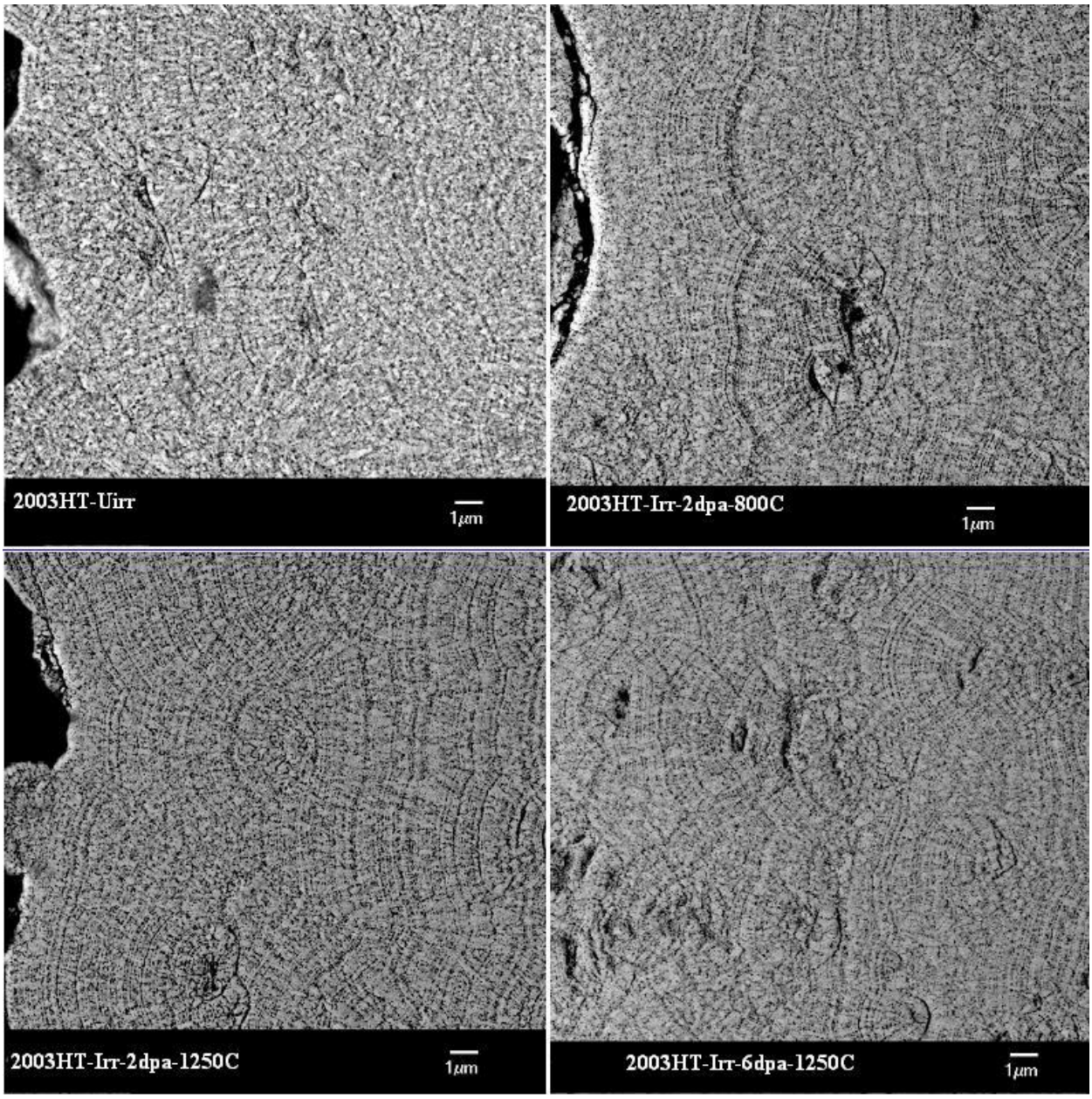

Fig. 15. Microstructure of Sample 2003 HT.

4.0 Nanoindentation Hardness and Elastic Modulus Measurements

4.1 Unirradiated Specimen Nanohardness and Modulus

The nanohardness and the elastic modulus were measured for all the unirradiated specimens using an MTS Nanoindenter XP system at room temperature. A final depth limit of 500 nm was selected for all the sample runs. The results of the nanoindentation measurements are summarized in Table 4.

Table 4. Results of Nanoindentation on unirradiated specimens

Sample Lot	Nanohardness	Nanohardness Std Deviation	Modulus (GPa)	Modulus Std Deviation	% Reduction in Hardness (Post HT)	% Reduction in Modulus (Post HT)
3002	29.98	0.96	350.5	21.11	-	-
3002HT	28.10	2.95	341.7	17.84	6.3	2.5
3010	29.20	0.84	366.5	7.40	-	-
3010HT	24.94	1.73	340.6	18.75	14.5	7.0
2003HT	18.62	0.56	240.2	11.85	-	-
2048HT	25.98	2.05	327.9	13.96	-	-

A comparison of the hardness and elastic modulus of the as-fabricated and heat-treated samples indicated that, with grain growth resulting from heat-treatment, the nanohardness and modulus values of the ZrC decreased. Although the phenomenon of reduction in the hardness seems to be similar to that observed in most metals, where large grain size reduces the material hardness and mechanical strength, application of the theory of dislocation motion linked to reduction in disordered obstacles, such as grain boundaries, is still unclear for ceramics such as ZrC and would require a further detailed theoretical analysis. Figures 16 and 17 show typical load versus displacement curves for samples 3002-3002HT and 3010-3010HT respectively, as recorded during the nanoindentation runs.

A quick comparison of average nanohardness values of heat-treated 2048HT, 2003HT, 3010HT and 3002HT samples indicates that the nanohardness of 2048HT and 3010HT lies roughly between those of 3002HT and 2003HT, further confirming the presence of a carbon-rich interlayer in these samples. A comparison of the modulus also reveals a slight reduction in 3010HT and 2048HT, compared to 3002HT, which could be attributed to the presence of carbon embedded between adjacent grains. The values of both nanohardness and modulus of sample 2003HT indicate a higher degree of softening in carbon-rich ZrC. However, it is noted here that the results of the nanoindentation have to be interpreted conservatively since the exact position of the indentation (relative to the center of the grain) cannot be controlled in materials with fine grain structures and may often require a large number of data points. The data is also expected to deviate on account of the substrate effects in thin samples.

Figure 18 shows the variation of nanohardness with the C/Zr ratio, as reported by He et. al. [4] with additional data points from the current work. The nominal C/Zr ratios reported by JAEA were used to plot the data points from the current work. It is seen in the graph that the hardness of ZrC reaches a maximum in the slightly carbon deficit range (C/Zr~0.8 to 1.0, hypostoichiometric composition) and decreases with increasing carbon content.

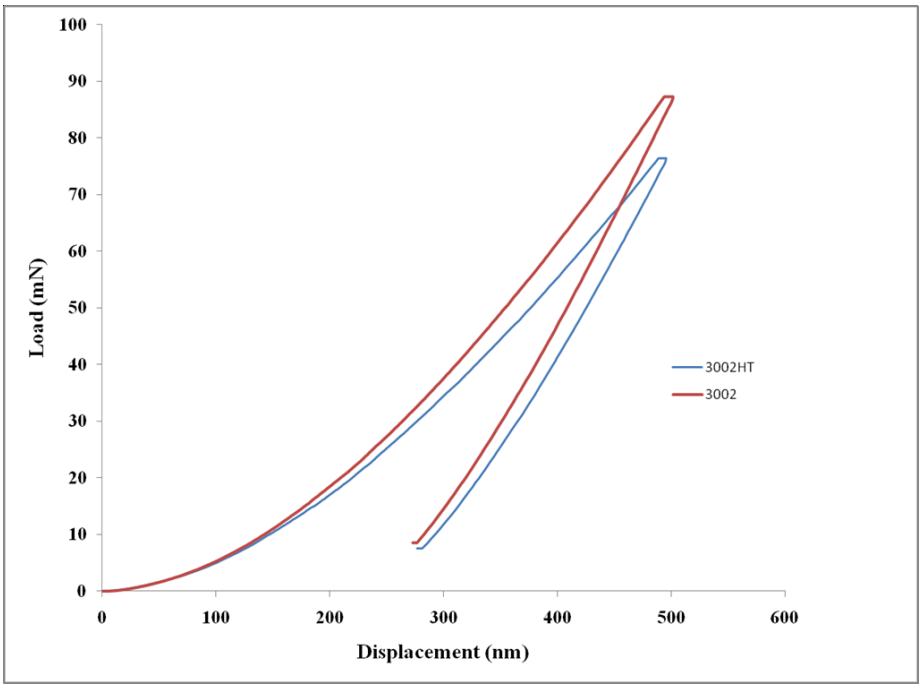

Fig. 16. Load vs. displacement curve showing post heat-treatment change in modulus in Sample 3002.

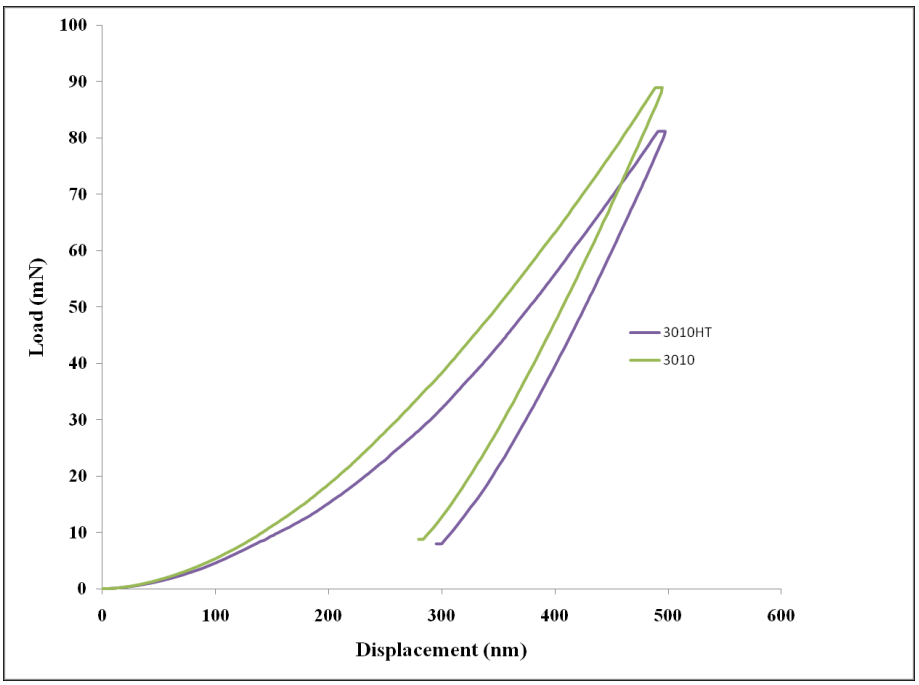

Fig. 17. Load vs. displacement curve showing post heat-treatment change in modulus in Sample 3010.

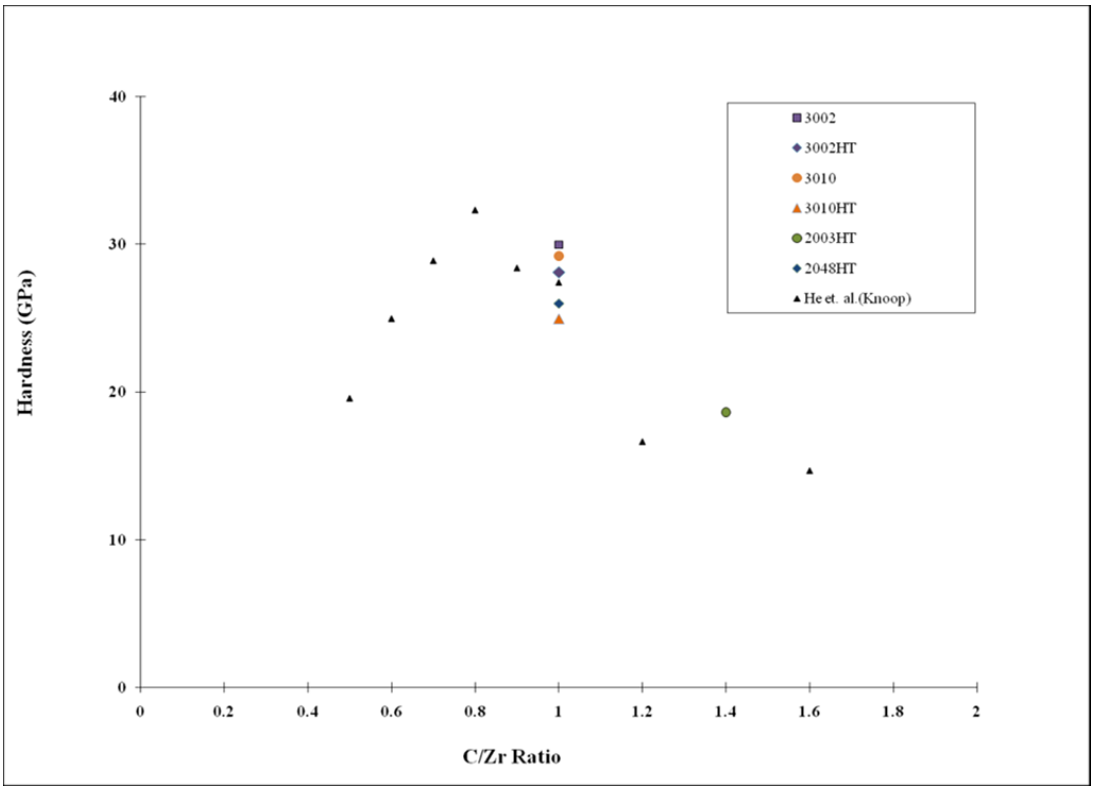

Fig. 18. Variation of hardness with C/Zr ratio

4.2 Irradiated Specimen Nanohardness and Modulus

The results of the nanoindentation tests on the irradiated samples are listed in Table 5. Post-irradiation measurements indicated that the hardness and modulus had decreased in most samples indicating irradiation induced softening. This is in contrast to some of the data previously reported in the literature, where a 10-15% increase in the hardness has been reported [5]. The reduction in hardness and modulus were significant at the highest dose of 6 dpa and only modest at 2 dpa. Figures 19 and 20 show the measured changes in nano-hardness and modulus in the samples, respectively.

The as-fabricated samples (3002 and 3010) appeared to have softened the most, especially at the highest irradiation dose (6 dpa). Sample 3002 showed a total change of ~68% in the measured hardness and ~50% in the modulus. This anomaly could not be explained as the microstructure did not reveal any noticeable changes such as microcracks or large scale grain enhancement to warrant such a drastic reduction in the hardness. A careful investigation of the raw data indicated highly consistent and repeatable measurements putting to rest any speculation on changes in test setup or the parameters during the measurements. Sample 3010 irradiated to 6 dpa showed ~ 16% reduction in hardness and ~17% reduction in the modulus.

The reduction in both modulus and hardness in the heat-treated samples were comparatively lower than the as-fabricated samples. However, most of them exhibited a similar trend, where the hardness decreased with increasing dose. Sample 3002HT, where a homogenous grain structure

was observed, had the least reduction in hardness and modulus at the highest dose. The changes in hardness and modulus were a modest 2.5% and 2.8%, respectively.

As an exception to other observations sample 3010 HT (irradiated to 2 dpa at both 800 and 1250°C) showed a modest increase in the hardness and modulus. However, the reduction trend resumed at the highest dose of 6 dpa.

Although grain growth and evolution of pores and microcracks may be construed as possible causes for this drastic reduction, microstructural observations did not bare evidence to this phenomenon on a large scale as predicted by these measurements. It is important to note here that the hardness of ZrC is highly dependent on the orientation of the indenter and the ZrC crystallographic orientation. A variation in the measured values is hence expected, as there is no particular order of orientation in these coatings, but such drastic changes could not be explained at present. It is expected that further investigations using other characterization tools, such as transmission electron microscopy, could possibly link the microstructure with these measurements and address this anomaly.

Table 5. Results of Nanoindentation on irradiated samples.

Sample Lot	T_{irr} (°C)	Dpa	Hardness	Std Dev. (Hardness)	*Change in Hardness (%)	Modulus (GPa)	Std Dev. (Modulus)	*Change In Modulus (%)
3002HT	Unirr	-	28.1	2.95	-	341.7	17.84	-
	800	2	26.9	5.01	4.3	339.1	46.36	0.8
	1250	2	25.5	1.51	9.2	271.5	11.22	20.5
	1250	6	27.4	4.00	2.5	332.2	24.60	2.8
3002	Unirr	-	29.9	0.93	-	350.5	21.11	-
	800	2	27.1	2.65	9.4	304.3	30.21	13.2
	1250	2	27.3	1.55	8.7	332.1	12.14	5.2
	1250	6	9.51	1.38	68.2	177.6	13.52	49.3
3010HT	Unirr	-	24.9	1.73	-	340.6	18.75	-
	800	2	25.9	1.89	-4.0	317.5	11.09	6.8
	1250	2	27.7	1.71	-11.2	352.0	15.30	-3.3
	1250	6	21.3	1.45	14.5	290.2	8.84	14.8
3010	Unirr	-	29.2	0.83	-	366.5	7.39	-
	800	2	24.3	2.09	16.8	292.6	10.80	20.2
	1250	2	-	-	-	-	-	-
	1250	6	24.5	2.44	16.1	302.2	16.97	17.5
2048HT	Unirr	-	25.9	2.05	-	327.9	13.96	-
	800	2	25.9	1.11	0.0	315.8	8.895	3.7
	1250	2	25.2	2.37	2.7	325.0	14.41	0.9
	1250	6	19.4	2.28	25.1	262.8	16.50	19.9
2003HT	Unirr	-	18.6	0.56	-	240.2	11.85	-
	800	2	18.4	1.43	1.1	196.7	12.04	18.1
	1250	2	17.7	1.13	4.8	224.8	9.07	6.4
	1250	6	14.4	1.93	22.6	197.9	40.18	17.6

* *With reference to unirradiated specimen data*
* *Negative values indicate hardening*

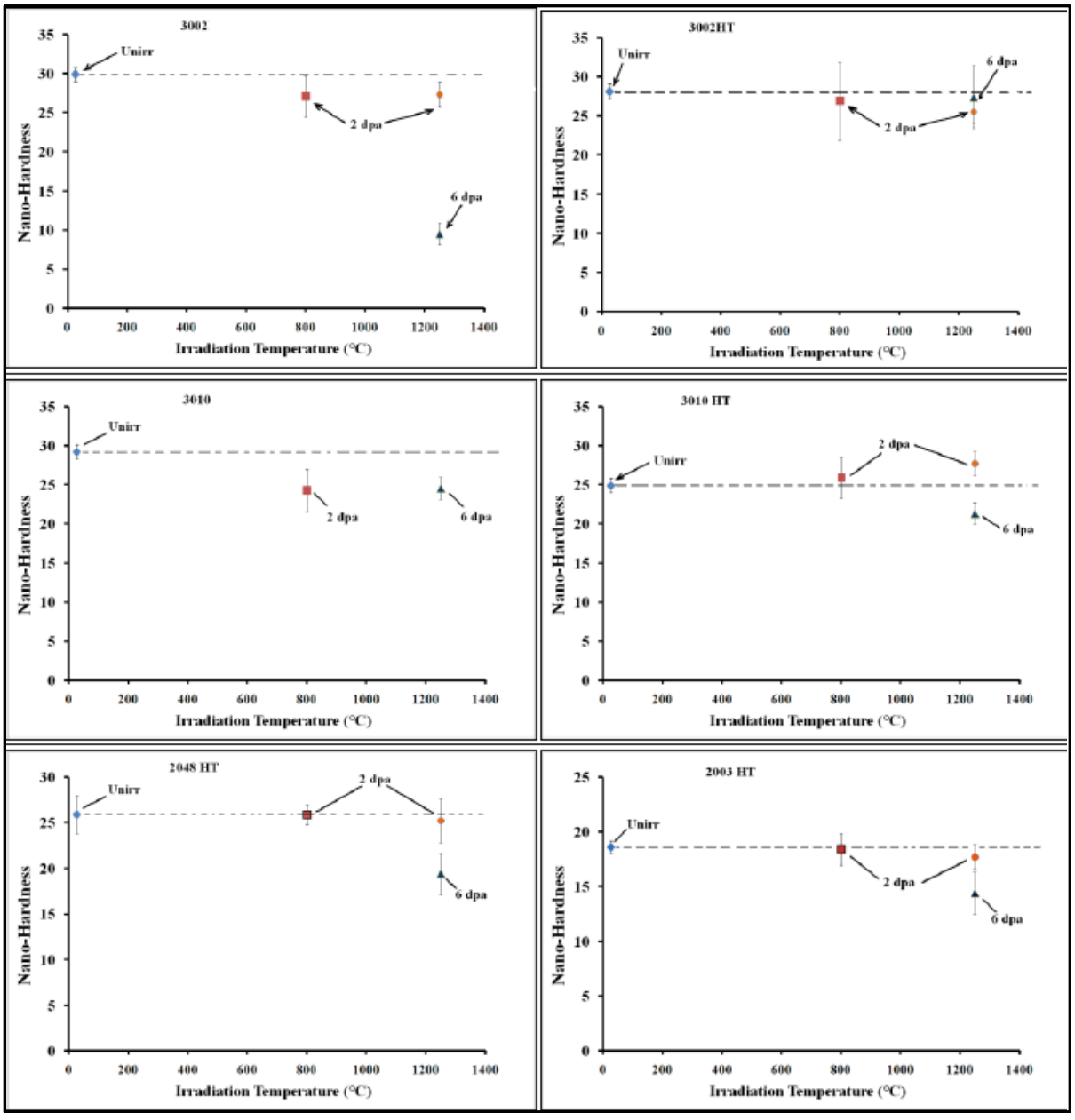

Fig. 19. Variation of Hardness with dose and irradiation temperature.

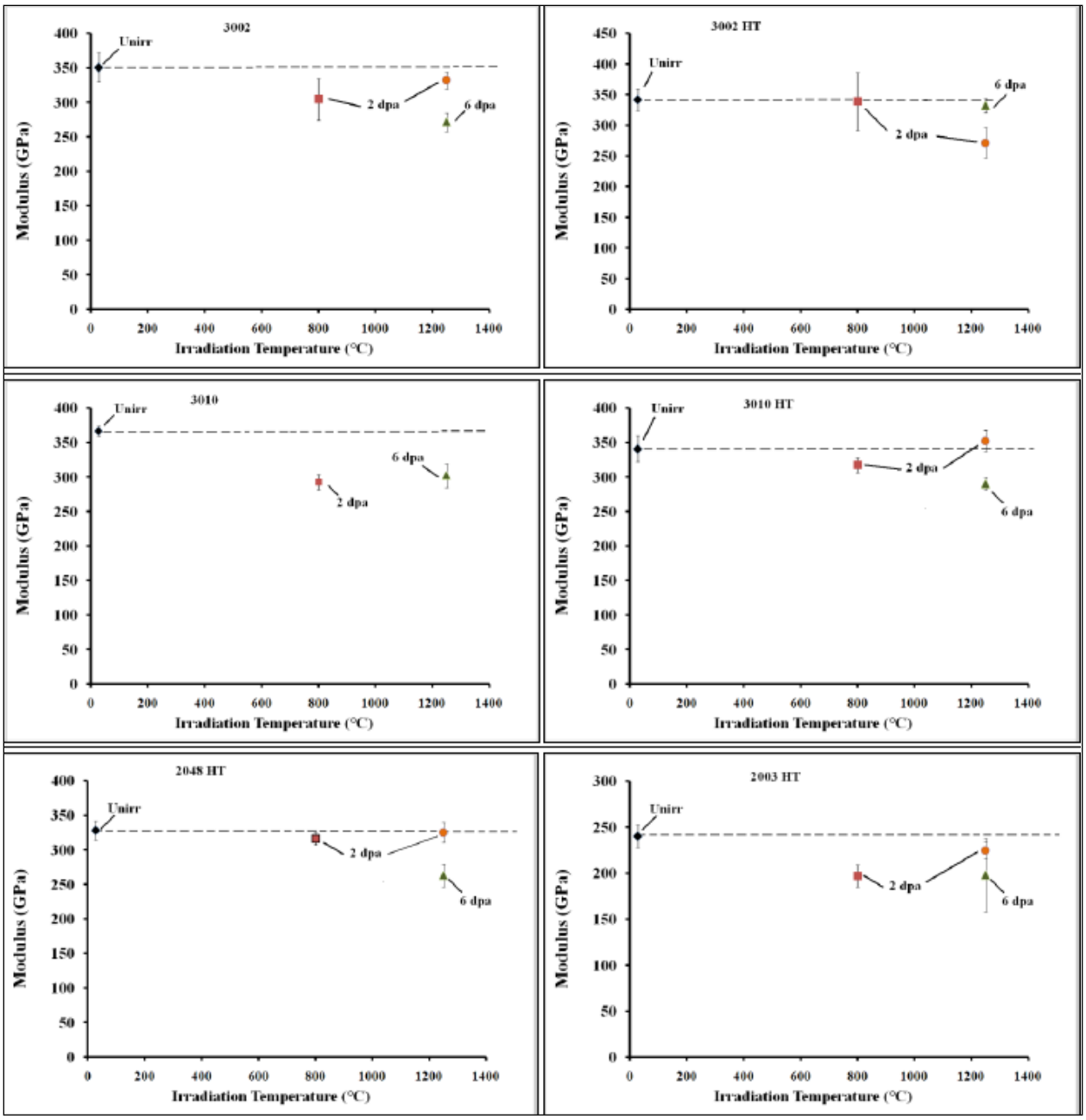

Fig. 20. Variation of Modulus with dose and irradiation temperature.

4.3 Conclusions of the Nanoindentation Measurements

In the unirradiated sample, the nanohardness and modulus of ZrC decreased with the grain growth resulting from heat-treatment. The nanohardness and modulus of ZrC also reduced due to the presence of relatively softer carbon-rich layers between coating interlayers, significantly softening the bulk material.

The nanohardness and modulus decreased in irradiated samples irrespective of their composition or homogeneity, indicating major degradation in the post-irradiation nano-mechanical properties. Barring some anomalies, the reduction was not as significant in samples irradiated to 2 dpa

compared to 6 dpa. The as-fabricated sample 3002 exhibited the largest change in modulus and hardness. The heat-treated sample 3002HT showed the least change in modulus and hardness at the highest dose (6 dpa). These observations of drastic softening are in contrast to the data reported in the literature and could not be currently explained in terms of the observed microstructures.

5.0 References

1. J. Aihara, S. Ueta, A. Yasuda, H. Ishibashi, T. Takayama, K. Sawa, and Y. Motohasi, "TESM/STEM observation of ZrC-coating layer for Advanced High Temperature Gas-cooled Reactor fuel", *J. Am. Ceram. Soc.*, 90, 12, 2007.
2. J. Aihara, S. Ueta, A. Yasuda, H. Ishibashi, T. Takayama, K. Sawa, and Y. Motohasi, "TESM/STEM observation of ZrC-coating layer for Advanced High Temperature Gas-cooled Reactor fuel , Part II", *J. Am. Ceram. Soc.*, 92, 1, 2009.
3. J. Aihara, S. Ueta, A. Yasuda, H. Takeuchi, Y. Mosumi, K. Sawa, and Y. Motohasi, "Effect of heat-treatment on TEM microstructrues of Zirconium Carbide coating layer in fuel particle for advanced high temperature gas cooled reactor", *Mat. Transc.*, 50, 11, 2009.
4. X. M. He, L. Shu, H.B. Li, H.D. Li and S.T. Lee, "Structural characteristics and hardness of zirconium carbide films prepared by tri-ion beam assisted deposition", *J. of Vacuum Science & Technology A, Vacuum Surfaces & Films*, 16**,** 4, 1998.
5. L. L. Snead, Y. Katoh, and S. Kondo, "Effects of Fast Neutron Irradiation on Zirconium Carbide", J. Nuclear Materials, 339, 2-3, 2010.